

## NOVEL NANOSIZED FRICTION MODIFIERS FOR ENGINE, GEARBOX AND ROLLING BEARINGS LUBRICANTS

*Adolfo Senatore\**, *Maria Sarno*, *Paolo Ciambelli*

<sup>1</sup>Department of Industrial Engineering, NANO\_MATES Research Centre  
University of Salerno, via Giovanni Paolo II, 132  
I-84084 Fisciano, Salerno, ITALY

**Abstract:** In this paper the tribological performances of graphene oxide nanosheets in mineral oil under wide spectrum of conditions, from boundary and mixed lubrication to elastohydrodynamic regimes, are reported. Nanosheets of graphene oxide prepared by a modified Hummer method have been dispersed in Group I mineral oil. The formulated lubricant has been tested through a ball on disc setup tribometer to quantify the friction reduction with respect to the base mineral oil. The good friction and anti-wear properties of the graphene-oil mixture may possibly be attributed to the small structure of the nanosheets and their extremely thin laminated structure, which offer lower shear stress and prevent direct interaction between metal asperities in engine applications as well as gearbox environment. The results clearly prove that graphene platelets in oil easily form protective film to prevent the direct contact between steel surfaces and, thereby, improve the frictional behaviour of the base oil. This evidence is also related to the frictional coefficient trend in the boundary regime. Furthermore, hybrid organic-inorganic nanocomposites with different composition were successfully tested as antifriction and antiwear additives for grease lubricants as potential breakthrough media in rolling bearings applications.

**Keywords:** graphene oxide, nanosheets, nanosized friction modifier, wear reduction, grease lubricant, hybrid nanoadditives.

### 1. INTRODUCTION

In the field of tribological applications, nanoparticles as additives in base oil have been extensively investigated. These studies refer to synthesis and preparation of nanoscale particles, and their tribological properties and friction reduction mechanisms. It has been found that when the nanoparticles were added to base oil, the extreme-pressure property and load-carrying capacity were improved and friction coefficient was decreased.

In the past few years, nested spherical supra-molecules of metal dichalcogenide have been synthesized by reaction of metal oxide nanoparticles with H<sub>2</sub>S at elevated temperatures. Because of their nested fullerene-like structure, these species are known as inorganic fullerene-like (IF) nanoparticles. The IF nanoparticles exhibited improved tribological behaviour compared to the micro-scale platelets for their robustness and flexibility. The tribological properties of fullerene-like nanoparticles as additive to liquid lubricants were studied in [1-4].

Recently, due to high load-bearing capacity, low surface energy, high chemical stability, weak

intermolecular, and strong intramolecular bonding, nanocarbon materials have received a great deal of attention by tribology researchers. In recent years, due to their unique structure and remarkable properties, graphene platelets have been the focus of interest in studies on practical applications. However, few studies on the tribological applications of graphene platelets have been reported so far. A number of researchers have reported that graphite [5] and some graphite derivatives [6,7] as well as other lubricant materials [8-10] together have the above desirable properties. Lin et al. [11] investigated the tribological properties of graphite nanosheets as an oil additive. These materials are characterized by weak interatomic interactions between their layers (Van der Waals forces), low-strength shearing [12]. In [13], the tribological behaviours of graphene sheets modified by oleic acid and dispersed in lubricant oil were investigated using a four-ball tribometer.

Huang et al. [14] investigated the tribological properties of graphite nanosheets as an oil additive. They found that the frictional behaviour and anti-wear ability of lubricating oil were improved when

---

\* Corresponding author: a.senatore@unisa.it

graphite nanosheets were added to the paraffin oil at the optimal concentration.

In particular, to ensure uniform dispersion without any agglomeration of the graphene oxide (GO) in the base oil, taking advantage of the surface  $-OH$  and  $-COOH$  introduced during the GO preparation, a functionalization with long chain compounds (i.e. aliphatic amine to obtain the amide derivative) enhances the dispersion in non-polar solvents [11].

On the other hand, the additives such as carbon and even more, if functionalized with  $-OH$  and  $-COOH$  groups that increase their polarity, can be dispersed through the use of a dispersant [13], avoiding further chemical reactions and using a methodology well known to the lubricant industry.

In the present study the tribological behaviour of graphene nanosheets in Group I base mineral SN150 was investigated under a very wide spectrum of conditions, i.e. from boundary and mixed lubrication to the elastohydrodynamic (EHL) regimes. To explore the performances of the nanosheets in the lubricating fluid, a rotational tribometer with a ball on disc setup has been employed.

Raman analysis on the steel ball worn surfaces was performed to investigate the presence of graphitic material on the mating surfaces after tribological tests, in order to verify the formation of a protective film on the rubbing surfaces due to the additive.

Furthermore, a new synthetic strategy to obtain hybrid organic-inorganic oleylamine@MoS<sub>2</sub>-CNT nanocomposites with different compositions is reported in the second part of this paper. Such materials were dispersed in grease lubricants to evaluate their anti-friction and anti-wear properties. The tribological characterization provides useful data to consider the inclusion of such novel materials in lubricant grease for rolling bearings from high- to very-high hertzian contact pressure conditions.

## 2. GRAPHENE OXIDE NANOSHEETS IN OIL LUBRICANT

### 2.1. Nanosheets preparation and characterization

#### 2.1.1. Materials

Graphene Oxide (GO) nanosheets were prepared at the laboratories of the Nano\_Mates centre by a modified Hummer method [15]. The oxidation of graphite particles were obtained from Lonza [16,17] to graphitic oxide accomplished with water-free mixture of concentrated sulfuric acid, sodium nitrate and potassium permanganate. The

entire process requires less than two hours for completion at temperatures below 45 °C. With an aid of further sonication step, the oxidized graphite layers were exfoliated from each other. Then 30% H<sub>2</sub>O<sub>2</sub> was added to the suspension to eliminate the excess MnO<sub>4</sub><sup>-</sup>. The desired products were rinsed with deionized water. The remaining salt impurities were eliminated with resinous anion and cation exchangers. The dry form of graphitic oxide was obtained by centrifugation followed by dehydration at 40 °C.

A polyisobutyl succinic acid-polyamine ester was sonicated with the GO nanosheet in base oil to provide dispersion stability of the additive; the weight ratio GO/dispersant was 3.5. The dispersant has a polar head that attaches itself to the solid particles and a very long hydrocarbon tail that keeps it suspended in oil.

Once several dispersant polar heads have attached themselves to a solid particle, the dispersant can no longer combine with other particles to form large aggregates, enwrapping one nanoparticle to repel another and thereby form a uniform suspension.

#### 2.1.2. Characterization methods

Scanning electron microscopy (SEM) pictures were obtained with a LEO 1525 microscope. The samples, without any pre-treatment, were covered with a 250 Å thick gold film using a sputter coater (Agar 108 A). Raman spectra were obtained at room temperature with a microRaman spectrometer Renishaw inVia with 514 nm excitation wavelength (laser power 30 mW) in the range 100–3000 cm<sup>-1</sup>. Optical images were collected with the optical microscopy connected on line with the Raman instruments. XRD measurements were performed with a Bruker D8 X-ray diffractometer using CuK $\alpha$  radiation. Micro X-ray diffraction patterns were obtained by an  $\mu X$  – ray diffractometer (Rint Rapid, Rigaku Corporation).

### 2.2. Tribological tests description

In this study, the investigated tribopair was composed by an upper rotating disc and a lower ball specimen completely immersed in a temperature-controlled lubricant bath in line with the features of the used tribometer, Wazau TRM100. The upper element of the tribopair was a X155CrVMo12-1 steel disc, 60 HRC, roughness Ra = 0.50  $\mu$ m and 105 mm diameter, the lower one was a X45Cr13 steel ball, 52-54 HRC, 8 mm in diameter.

The tribological test rig used for exploring the effectiveness of nanosized friction modifiers is the Wazau TRM 100 with the ball-on-rotational disc setup as in the drawing in Figure 1. The two mating materials are: (ball) steel X45Cr13, hardness: HRC 52-54, diameter: 8 mm, mean surface roughness: 0.2  $\mu\text{m}$ ; (disc) steel X155CrVMo12-1, hardness: HRC 60, diameter: 105 mm, mean surface roughness: 0.5  $\mu\text{m}$ .

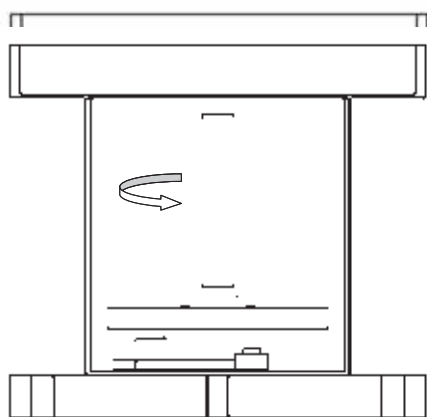


Figure 1. Tribopair functional scheme

The normal force to the ball-disc contact was delivered by a lever system and could be varied in the range of 0-100 N; its value was measured through a load cell placed under the specimen holder. The following average hertzian pressures were used at the ball/disc interface with normal load given in brackets: 1.17 GPa (30 N), 1.47 GPa (60 N), 1.68 GPa (90 N). The tests were performed for three different temperatures, 25, 50 and 80  $^{\circ}\text{C}$ , and the lubricant average temperature has been kept constant through a NiCr-Ni-thermocouple in the oil reservoir

and an electric resistance driven by a digital controller. This control system allows a control range from room temperature up to 100  $^{\circ}\text{C}$ .

Speed-sweep tests at constant load on broad sliding speed range have been performed to cover different lubrication regimes with an aim to minimize the modification of the tribopair steel surfaces. For this reason, the time extension of each test was limited to 16 minutes. The disc speed rose up to 2.20 m/s in the first 4 minutes and dropped to zero in the following 4 minutes. This speed pattern was repeated twice. The current design of this experiment allowed obtaining of a complete Stribeck frictional graph.

The tests were performed for three different temperatures, i. e. 25, 50 and 80  $^{\circ}\text{C}$ . All the samples have been stirred before each test for 20 minutes by means of a Turrax T 25 Digital homogenizer with adjustable speed. No chemical dispersant agents were used in order to explore the benefits coming from the pure addition of nanoparticles.

Tests were also carried out to analyse the influence of GO addition to the base oil on wear behaviour of the steel ball/disc tribopair through steady state rubbing tests, see section 3.2.2. For these tests, constant values for average hertzian pressure, temperature and speed were chosen.

### 2.3. Graphite and GO characterization

Graphite chips and GO nanosheets are shown in Figures 2a, 2b and 2c, 2d, respectively. The images at higher magnification (Figures 2b and 2d), evidence the loss of the chips structure of original graphite to GO transparent and thin flakes.

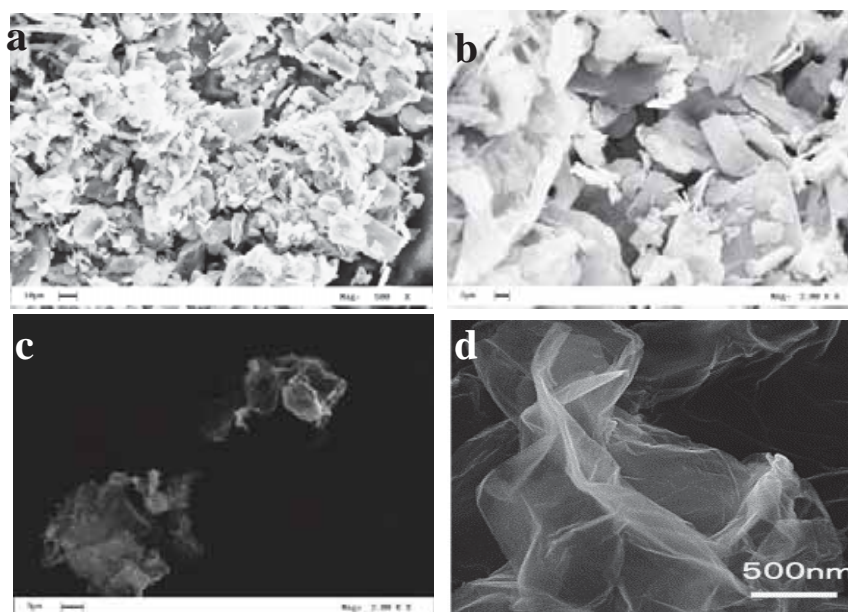


Figure 2. Graphite (a, b), GO (c, d)

## 2.4. Tribological results

### 2.4.1. Friction coefficient

The measured data are presented according to the Stribeck curves representation, i. e. friction coefficient vs. sliding speed. The results obtained for the lubricant sample formulated with GO nanosheets for different level of temperature and average hertzian contact pressure are shown below. The main proper-

ties of the base oil were: kinematic viscosity, 29.7 cSt at 40 °C, 5.1 cSt at 100 °C; density at 20 °C, 0.87 kg/m<sup>3</sup>.

A comparison between the samples SN150 with 0.1 w. t.% GO and the SN150 base oil shows that reduction of the friction coefficient for the sample with graphene nanoparticles is remarkable, Figure 3 a–f.

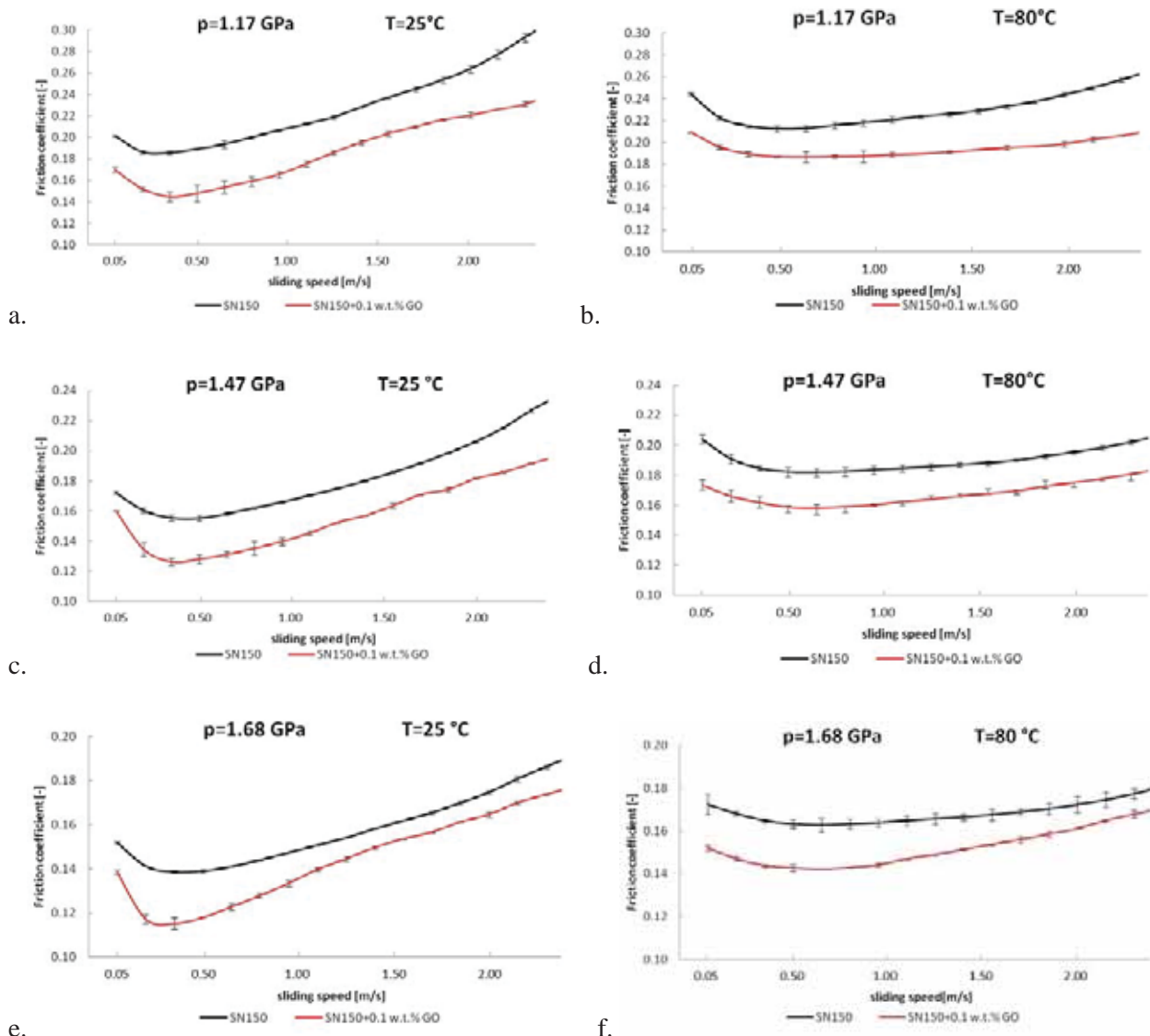


Figure 3. Stribeck curves comparison from the sweep-speed test (SN150 – black, SN150 with 0.1 w.t.% GO – red)

These results show a decrease of the friction coefficient for increasing average hertzian contact pressure for the formulated sample; the same behaviour has been observed for the base oil according to a point-contact studied effect: the shear stress increases less in proportion to the contact pressure; this leads to a slight reduction of friction [18]. As expected, for a given sample, the minimum of the Stribeck curve moves right for the increasing

temperature due to the lower viscosity. Additionally, for each sample, the CoF increased with the temperature at a given level of speed and contact pressure. This observation could mainly be addressed to the effect of the lower lubricant viscosity and the ensuing GO precipitation at higher temperature.

These Stribeck curves at three levels of average hertzian pressure (1.17 GPa, 1.47 GPa and



1.68 GPa) show a shape with a well-developed minimum, which is considered as transition from a mixed lubrication regime to EHL regime for increasing speed [19]. This frontier divides the region with concurrent phenomena of solid-to-solid contacts, adhesion and interaction between friction modifier additives and steel surface (mixed lubrication) from the other with predominant viscous stress and elastic deformation of the tribopair surfaces (EHL). For instance, the transition appears in the speed range 0.30–0.40 m/s for the test at 25 °C and 0.50–0.60 m/s at the higher temperature, 80 °C.

These tests confirm that using graphene nanoparticles in lubricants enhances the friction reduction in the boundary, mixed and EHL lubrication regimes.

For instance, with average contact pressure of 1.17 GPa and temperature in the range 25–80 °C, the average friction coefficient decreased by 20% of

the base lubricant value, but a similar average reduction could be observed for all the combinations of the operating conditions. Even in the heaviest test conditions (high pressure and temperature) and in fully developed EHL regime where the viscous stress is prevalent, the CoF reduction is greater than 8% (Figure 5f).

1-hour sliding tests were also performed to analyse the influence of the progressive wearing of the mating materials on the friction coefficient (Figure 4). The average friction coefficients measured during these steady state tests are presented in Tables 1 and 2. According to ISO/IEC Guide 98-3:2008, the average friction coefficients are presented with expanded uncertainty equal to  $5 \cdot 10^{-3}$ , coverage factor  $k = 2$ .

The lubrication regimes in these tables and Figure 4 are identified according to the results of the Stribeck curves.

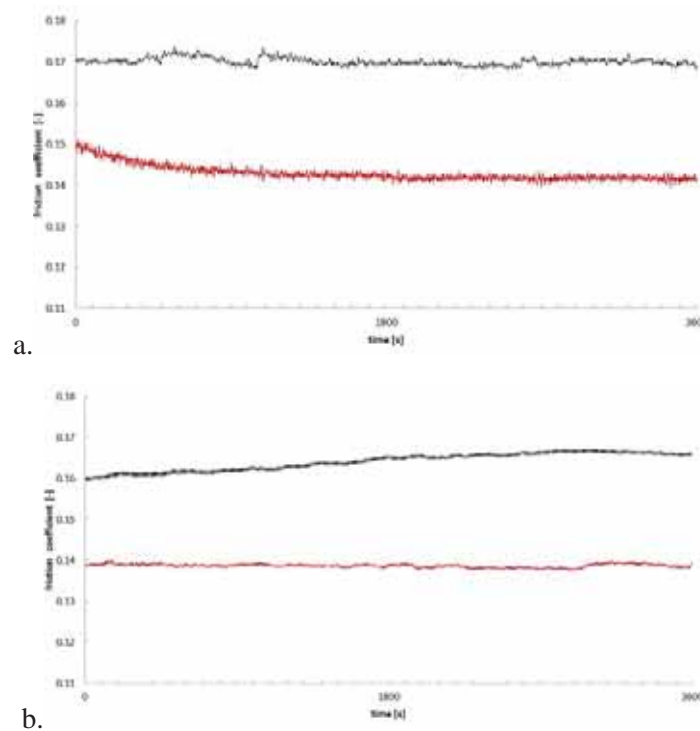


Figure 4. Friction coefficient in 1-hour steady state test with average hertzian contact pressure 1.68 GPa and oil temperature 80 °C: (a) sliding speed 5.0 mm/s, boundary regime; (b) sliding speed 0.50 m/s, mixed regime (SN150 – black, SN150 with 0.1 w.t.% GO – red)

Table 1. Friction coefficient in steady boundary and EHL lubrication conditions at 25 °C

Sample	Average hertzian contact pressure 1.68 GPa Oil temperature 25 °C		Difference
	Average friction coefficient at 5.0 mm/s sliding speed Boundary regime	Average friction coefficient at 0.50 m/s sliding speed EHL regime	
SN150 – Base oil	0.158	0.142	Benchmark
SN150 with 0.1 w.t.% GO	0.136	0.118	-14%    -17%

Table 2. Friction coefficient in steady boundary and mixed lubrication conditions at 80°C

Sample	Average hertzian contact pressure 1.68 GPa Oil temperature 80 °C		Difference	
	Average friction coefficient at 5.0 mm/s sliding speed Boundary regime	Average friction coefficient at 0.50 m/s sliding speed Mixed regime		
SN150 – Base oil	0.173	0.163	<i>Benchmark</i>	
SN150 with 0.1 w. t. % GO	0.141	0.139	-18%	-15%


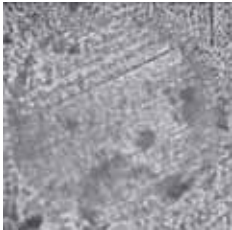
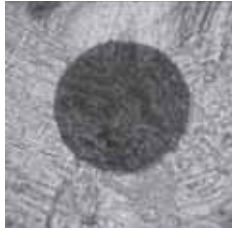
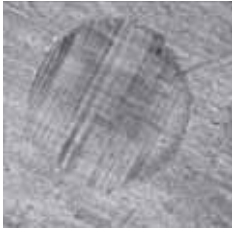
#### 2.4.2. Wear parameter

At the end of each 1-hour steady state test, the worn surface of the steel ball has been measured with an optical microscope to acquire the wear scar diameter (WSD). The WSD values are reported in Tables 3–4. According to ISO/IEC Guide 98-3:2008, the wear scar diameter (WSD) results are listed with expanded uncertainty equal to 20 µm, coverage factor k = 2.

The anti-wear property of GO as an additive for liquid lubricants has been clearly exhibited in all the lubrication regimes.


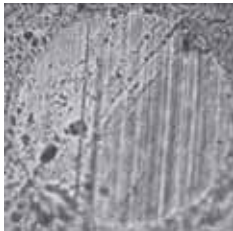

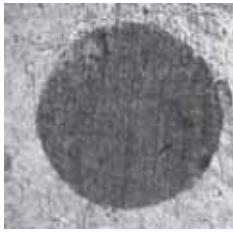
In particular, the presence of graphene oxide in the formulated samples, leading to the reduction of the ball wear scar diameter data equal to 12%, 27% and 30% in boundary, mixed and EHL regime, respectively.

Table 3. Wear scar diameter (WSD) after 1-hour boundary and EHL regime test at 25 °C

Sample	Average hertzian contact pressure 1.68 GPa Oil temperature 25 °C		Difference	
	Ball wear scar diameter [µm] at 5.0 mm/s sliding speed Boundary regime	Ball wear scar diameter [µm] at 0.50 m/s sliding speed EHL regime		
SN150 – Base oil	 600	 900	<i>Benchmark</i>	
SN150 with 0.1 w.t.% GO	 530	 630	-12%	-30%

*Pictures not to scale*

Table 4. Wear scar diameter (WSD) after 1-hour boundary and mixed regime test at 80 °C

Sample	Average hertzian contact pressure 1.68 GPa Oil temperature 80 °C		Difference
	Ball wear scar diameter [ $\mu\text{m}$ ] at 5.0 mm/s sliding speed Boundary regime	Ball wear scar diameter [ $\mu\text{m}$ ] at 0.50 m/s sliding speed Mixed regime	
SN150 – Base oil	 620	 910	Benchmark
SN150 with 0.1 w.t.% GO	 540	 660	-13%    -27%

*Pictures not to scale*

### 2.5. Raman spectrum of the worn surface

In Figure 5 the Raman spectra of graphite and graphene oxide nanosheets are reported. In particular, in the spectrum of graphite, the most prominent features [20], the so-called G band appearing at  $1582\text{ cm}^{-1}$  [21] and the G' or 2D band at about  $2700\text{ cm}^{-1}$ , using 514 nm excitation wavelength, are collected. The G' band at room temperature can be fitted with two Lorentzian lines. A broad D-band, due to disorder or edge [22] of a graphite sample, can be also seen at about a half of the frequency of the G' band (around  $1350\text{ cm}^{-1}$

using 514 nm laser excitation). The oxide graphene shows, as expected, improved D band intensity and flattening of the 2D line and displays a shift to higher frequencies (blue-shift) of a broader G band [23]. In figure 5, the Raman Spectrum collected on the ball wear after a 2 hours test at  $p=1.68\text{ GPa}$ ,  $T = 25\text{ °C}$ ,  $v = 0.5\text{ m/s}$  is also reported. A notable fact is that the G band of this spectrum is located almost at the same frequency as that in the graphite, while the G' band exhibits a single Lorentzian feature and D-band results reduced, evidencing the presence of a thin carbon film (“tribo-film”) on the wear scar surface.

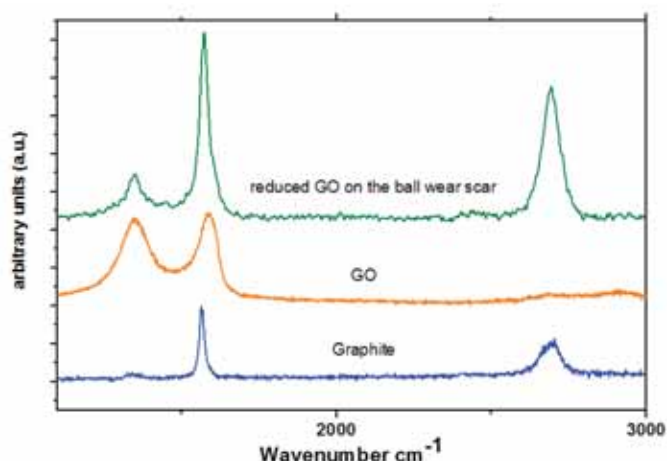


Figure 5. Raman spectra of Graphite, GO and reduced GO on the ball wear scar after 2-h sliding test

### 3. DISPERSION OF HYBRID ORGANIC-INORGANIC NANOADDITIVES IN GREASE

The development and use of these materials at the nanometric scale, with a different shape and morphology, such as fullerene-like materials [24–29] inorganic and carbon nanotubes [30–33], disulphide nano sheets and graphene [34–39] have shown better tribological properties, either in friction reduction or wear resistance, than bulk microsized disulphides and graphite. In order to conjugate and to enhance, through a unique synergy, the performances of these extraordinary materials at the nanoscale, the synthesis of hybrid-nanostructures, made by CNT and nanochalcogenides, has become an important goal not only in lubrication [40–43] but also in other research fields, such as energy conversion and storage [44–47], reinforced nanocomposites [48] and solar cells [49]. For these reasons, binary systems such as MoS<sub>2</sub>-coated carbon nanotubes have been recently synthesized by hydrothermal route [50–51], impregnation and annealing [38,52,53], electrodeposition [41]. Here we describe the main results from tribological test performed on dispersions of hybrid organic-inorganic oleylamine@MoS<sub>2</sub>-CNT nanocomposites in Lithium and Calcium based greases.

The synthetic strategy to obtain such hybrid organic-inorganic nanosized materials is explained in details in [54].

A new synthetic strategy to obtain hybrid organic-inorganic oleylamine@MoS<sub>2</sub>-CNT nanocomposites.

#### 3.1. Preparation of OA@MoS<sub>2</sub>-CNT nanocomposite.

30 mg of CNT were mixed with 0.4 g of (NH<sub>4</sub>)<sub>2</sub>MoS<sub>4</sub> in 18 ml of oleylamine and sonicated for 30 minutes. The red homogeneous dispersion was transferred to a three-necked spherical flask of 100ml, equipped with a water condenser. The reaction mixture was gradually (5 °C/min) heated to 360 °C and maintained at this temperature for 60 min under nitrogen atmosphere and magnetic stirring. The reactor was cooled to room temperature by removing the heating

mantle and the product was collected by centrifugation after washing with ethanol.

#### 3.2. Preparation of OA@CNT-MoS<sub>2</sub> nanocomposite.

An analogous procedure was used to produce CNT@MoS<sub>2</sub> nanocomposite with CNT in excess with respect to MoS<sub>2</sub>. In this case 0.18g of CNT were mixed with 0.06 g of (NH<sub>4</sub>)<sub>2</sub>MoS<sub>4</sub> in 18 ml of oleylamine.

#### 3.3. Preparation of dispersions in lubricant greases.

Different amounts of oleylamine@CNT-MoS<sub>2</sub> or oleylamine@MoS<sub>2</sub>-CNT nanocomposite were added to calcium-based grease NLGI2 (Ca NLGI2) and lithium-based grease NLGI3 (Li NLGI3) and their anti-friction and anti-wear performance have been tested. The compositions of samples are reported in table 5. The experimental details for the synthesis of OA@MoS<sub>2</sub>, used as reference nanoadditive, have been reported in a previous work [55].

#### 3.4. Transmission electron microscopy analysis.

In Figures 6 and 7, TEM images of OA@MoS<sub>2</sub>-CNT- and OA@CNT-MoS<sub>2</sub> are reported. Since both molybdenum and sulphur atoms have larger weight than the carbon atom, the MoS<sub>2</sub> results highly contrasted. In panels (a) and (b) of Figure 6, nanosheets (1 to 3) of MoS<sub>2</sub> dispersed in oleylamine are clearly visible. They have an average d space (002) of 6.7±2 Å<sup>39</sup>. On the other hand, it is very difficult to focus on CNT in this sample, as evidenced in the image of panel (c), where nanosheets of MoS<sub>2</sub> can be observed on the nanotubes external surface. CNTs dipped in an oleylamine matrix covered by MoS<sub>2</sub> nanosheets are clearly visible in Figure 7 for OA@CNT-MoS<sub>2</sub>. MoS<sub>2</sub> can deposit easily on the outer surface of the carbon nanotube matrix owing to the nearly identical crystal structure of graphite and layered MoS<sub>2</sub>. CNTs have 10-20 nm outer diameter and 4–12 carbon walls (Figure 7d) partially sheathed with 1-3 layer MoS<sub>2</sub> nanosheets (Figure 7c and Figure 1) [31].

Table 5. Composition of grease samples tested

Grease	Nanoadditive	Wt.% of nanoadditive
Ca NLG2	OA@MoS <sub>2</sub>	0.1
Ca NLG2	OA@MoS <sub>2</sub> -CNT	0.1
Ca NLG2	OA@CNT-MoS <sub>2</sub>	0.1
Li NLGI3	OA@MoS <sub>2</sub>	0.1
Li NLGI3	OA@MoS <sub>2</sub> -CNT	0.1
Li NLGI3	OA@CNT-MoS <sub>2</sub>	0.1



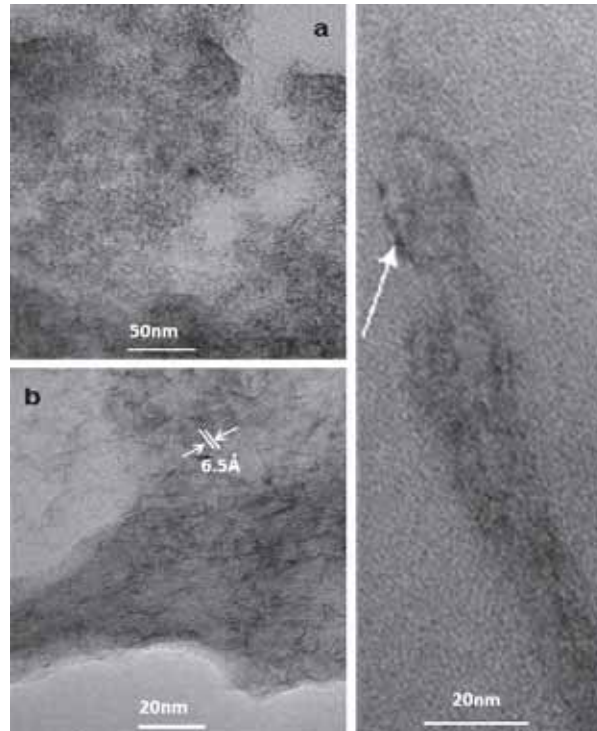


Figure 6. TEM images of OA@MoS<sub>2</sub>-CNT at different magnification

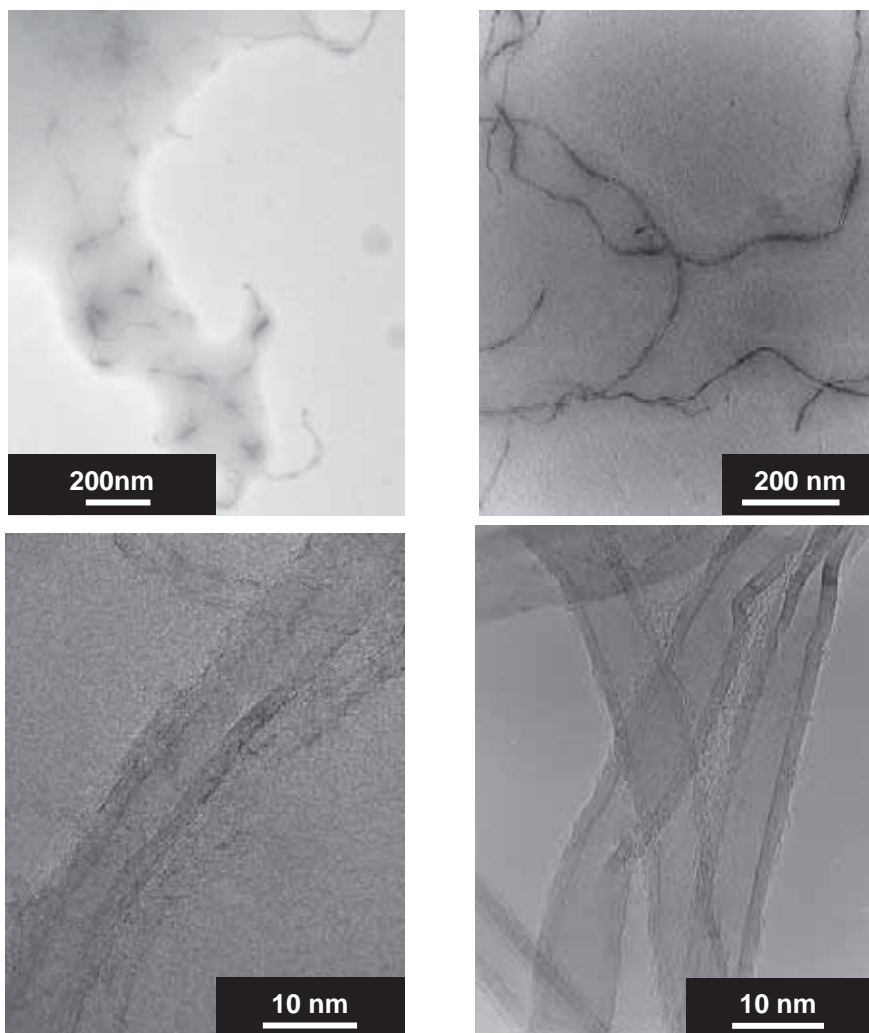


Figure 7. TEM images of OA@CNT-MoS<sub>2</sub> (a, b, c) and CNT (d) at different magnification

### 3.5. Tribological results

The experimental data are referred to steady sliding tests aimed at investigating two different lubrication regimes. A normal load level of 90 N has been applied to attain an average hertzian contact pressure around 1.7 GPa. The grease temperature has been kept constant at room level in each test. The relative motion between the steel ball and the disc was pure sliding at two speed levels: 5.0 mm/s and 0.50 m/s. According to the previous results achieved by the authors on Calcium and Lithium greases for the same tribopair geometry, average contact pressure and temperature, the boundary lubrication regimes and the mixed lubrication, as superposition of boundary and elastohydrodynamic lubrication (EHL) regimes were covered [35,56,57].

For each experiment, both the ball and the disk were pre-cleaned and the grease was then evenly pasted on the disk sliding path forming a layer with thickness of 2 mm at least. The test length was 60 minutes; thus, the actual sliding distance was 18 m and 1800 m for the speed of 5.0 mm/s and 0.50 m/s, respectively. The friction coefficient has been indirectly measured in real-time by means of a

torque sensor on the ball holder plate. The wear damage circle on the top of the steel ball was measured off line by optical microscopy.

The results of the friction tests, performed under the operating conditions described above, in both the investigated lubrication regimes are summarized in the Table 6. Tests were also performed to analyse the behaviour of the lubricating grease samples with regard to the wear damage of the steel ball surface. In particular, the worn surface of the steel ball has been analyzed by means of an optical microscope to measure the wear scar diameter (WSD), Table 7. According to the ISO/IEC Guide 98-3:2008, the expanded uncertainty of the frictional data and WSD measurements are  $5.0 \times 10^{-3}$  and 20  $\mu\text{m}$ , respectively, by assuming the coverage factor  $k = 2$ . Both in lithium and calcium greases, the addition of OA@MoS<sub>2</sub>-CNT (constituted essentially of MoS<sub>2</sub> nanosheets and few coaxial CNT-MoS<sub>2</sub> nanotubes coated by oleylamine) determines a reduction of friction and wear at ball-disc interface with respect to OA@MoS<sub>2</sub>. Better performances with regard to the frictional and wear reduction are offered by the samples with 0.1 w. t.% concentration of OA@CNT-MoS<sub>2</sub> in either calcium and lithium base greases.

Table 6. Friction coefficients in boundary and mixed regimes

Sample	Friction coefficient in Boundary regime [-]	Friction coefficient in Mixed regime [-]	Difference
Ca NLGI 2	0.110	0.100	Benchmark
Ca NLGI2 at 0.1 w.t.% of OA@MoS <sub>2</sub>	0.094	0.092	-15% -8%
Ca NLGI2 at 0.1 w.t.% of OA@MoS <sub>2</sub> -CNT	0.090	0.081	-18% -19%
Ca NLGI2 at <b>0.1 w.t.%</b> of OA@CNT-MoS <sub>2</sub>	0.083	0.080	<b>-25% -20%</b>
Li NLGI 3	0.090	0.090	Benchmark
Li NLGI3 at 0.1 w.t.% of OA@MoS <sub>2</sub>	0.081	0.080	-10% -11%
Li NLGI3 at 0.1 w.t.% of OA@MoS <sub>2</sub> -CNT	0.077	0.073	-14% -19%
Li NLGI3 at <b>0.1 w.t.%</b> of OA@CNT-MoS <sub>2</sub>	0.071	0.069	<b>-21% -23%</b>

Table 7. Wear results in boundary and mixed regimes

Sample	Ball wear scar diameter [ $\mu\text{m}$ ] Boundary regime	Ball wear scar diameter [ $\mu\text{m}$ ] Mixed regime	Difference
Ca NLGI 2	820	1200	Benchmark
Ca NLGI2 at 0.1 w.t.% of OA@MoS <sub>2</sub>	730	940	-11% -22%
Ca NLGI2 at 0.1 w.t.% of OA@MoS <sub>2</sub> -CNT	710	900	-13% -25%
Ca NLGI2 at 0.1 w.t.% of OA@CNT-MoS <sub>2</sub>	660	820	<b>-20% -32%</b>
Li NLGI 3	800	920	Benchmark
Li NLGI3 at 0.1 w.t.% of OA@MoS <sub>2</sub>	700	820	-13% -11%
Li NLGI3 at 0.1 w.t.% of OA@MoS <sub>2</sub> -CNT	690	800	-14% -13%
Li NLGI3 at 0.1 w.t.% of OA@CNT-MoS <sub>2</sub>	640	720	<b>-20% -22%</b>

This finding clearly shows an active role of the hybrid nanoadditive OA@CNT-MoS<sub>2</sub>, in which the inorganic core is made of coaxial CNT-MoS<sub>2</sub>

coated by oleylamine, in the decreasing of mechanical energy loss due to the shearing motion of the grease layers and in the interaction of the nanoaddi-

tive with tribopair rough surfaces as well. The enhanced tribological properties are probably due to the high resilience and elasticity of coaxial CNT-MoS<sub>2</sub> nanotubes [41] combined with the higher volume/weight ratio of the CNTs.

### 3.6. Discussion

An incessant literature dispute on the friction reduction mechanism introduced by nanoparticles as lubricant additives finds in the following list the more convincing physical explanations: rolling-sliding „rigid” motions together with flexibility properties [58–60], nanoadditive exfoliation and material transfer to metal surface to form the so-called „tribofilm” or „tribolayer” [1–3], electronic effects in tribological interfaces [3,61,62], surface roughness improvement effect or „mending” [63]; along with the more classical hypothesis of surface sliding on lower shear stress layers due to weak interatomic forces, valid also for micro-scale additives used for decades.

The experimental evidences of this paper could represent a proof of the presence of a tribological film of reduced graphene oxide which covers the whole worn surface of the steel ball. The since-start reduction of friction coefficient in both the Figs. 4 could be addressed to the surface rubbing through the low shear stress GO layers. The smoothly decreasing friction coefficient in boundary regime in Figure 4a may be related to the tribofilm development.

The GO 0.1 w. t.% concentration is quite lower than the usual one for inorganic nanoadditives [1,3] and carbon nanotubes [64] and in line with the previous studies in which oleic acid-modified graphene was used [13]. This feature is welcomed in the preparation of fully formulated engine or gearbox lubricants since the GO addition could only slightly modify a delicate equilibrium achieved by oil manufacturers between the essential and ubiquitous additives as antioxidant, viscosity modifier, pour-point depressant and other minors.

About the nanohybrid based grease lubricants, tests using pure CNT have been also performed to better understand the tribological behaviour of such materials composite additives. A physical mixture of CNT/oleylamine, in the right proportion, and calcium based grease, adding a total of 0.1 w. t.% of oleylamine+CNT, has been obtained by sonication. The mixture has been tested under boundary lubrication conditions, finding a -18% of reduction of the friction coefficient with respect to the pure Ca NLG2, while the ball wear scar diameter showed a difference of -15%. These results, better than that

exhibited by the OA@MoS<sub>2</sub> nanocomposite but worse than that shown by adding OA@CNT-MoS<sub>2</sub>, confirm a key role of the hybrid materials, characterized by an intimate connection between the oleylamine and the MoS<sub>2</sub>/CNT surfaces, resulting in an improvement of the additive dispersion in a quasi-solid matrix and determining better performances at the same weight concentration. It is noteworthy that another intrinsic advantage lays in the composite chemical nature of nanohybrid, to spend also under other test conditions. Moreover, lithium-based grease classified as NLGI3, according to the standard ASTM D 217, provides better tribological behaviour on the whole testing spectrum than the calcium-based grease, NLGI 2, as expected. The improved values of the frictional coefficient and wear parameter due to the addition of nanoadditives seem to replicate the differences found by testing the original commercial samples.

## 4. CONCLUDING REMARKS

The tribological tests confirm a good reduction of friction and wear parameters in boundary lubrication, mixed lubrication and EHL regimes achieved with mineral oils formulated with Graphene Oxide (GO) nanosheets prepared at the laboratories of the Nano\_Mates research centre, University of Salerno. For instance, with 1.17 GPa as average hertzian contact pressure and temperature in the range 25–80 °C, the average CoF decreased by more than 20% compared with the base lubricant value. The sliding tests in steady state conditions have shown an average reduction of CoF equal to 16%. The frictional reduction benefit has been proven at any level of oil temperature, contact pressure and sliding speed.

The best anti-wear result has been observed on the ball surface in the mixed lubrication and EHL regime, with the marked average decreasing around 30%. A tribological film of reduced GO nanosheets after the tribological test covers the ball wear scar.

The tendency toward the precipitation is a drawback for the formulated sample at the higher temperatures due to the lower lubricant viscosity.

The good friction and anti-wear properties of graphene sheets may be possibly attributed to their small structure and extremely thin laminated structure, which offer lower shear stress and prevent interaction between metal interfaces.

The results clearly prove that graphene platelets in oil easily form protective deposited films to prevent the rubbing surfaces from coming into

direct contact and, thereby, improve the entirely tribological behaviour of the oil.

New hybrid organic-inorganic nanocomposites, made by an inorganic core of CNT/MoS<sub>2</sub> coaxial nanotubes coated by oleylamine molecules was also successfully obtained by an innovative synthetic strategy by thermal decomposition of tetrathiomolybdate in the presence of oleylamine and multi-walled carbon nanotubes (MWCTN). Such hybrid nanostructures conjugate and enhance, through a unique synergy, the performances of CNT and nanochalcogenides, with the organic coating that promotes the compatibility in a-polar matrix (solvent, oil, grease). Nanohybrid composites, that are a potential candidate for a wide range of applications, were successfully tested as anti-friction and anti-wear additives. Nanocomposite samples were characterized by TEM, SEM TG-MS, Raman and XRD and successfully tested as antifriction and anti-wear additives for grease lubricants.

Future works will focus toward: methods for dispersion improvement of nanoparticles in oil; addition to other bases, fully formulated oils with standard additive compounds and grease for special applications (e.g. vacuum grease); search of optimal concentration and testing at lower contact pressure to verify the existence of activation threshold related to nanoparticles structure modification.

## 5. REFERENCES

- [1] R. Greenberg, et al., *The Effect of WS<sub>2</sub> Nanoparticles on Friction Reduction in Various Lubrication Regimes*, Tribology Letters, Vol. 17 (2004) 179–186.
- [2] L. J. Pottuz, et al., *Ultralow-friction and wear properties of IF-WS<sub>2</sub> under boundary lubrication*, Tribology Letters, Vol. 18 (2005) 477–485.
- [3] L. Yadgarov, et al., *Tribological studies of rhenium doped fullerene-like MoS<sub>2</sub> nanoparticles in boundary, mixed and elasto-hydrodynamic lubrication conditions*, Wear, Vol. 297 (2013) 1103–1110.
- [4] R. Rosentsveig, et al., *Fullerene-like MoS<sub>2</sub> Nanoparticles and Their Tribological Behavior*, Tribology Letters, Vol. 36 (2009), 175–182.
- [5] J. Wintterlin, et al., *Graphene on metal surfaces*, Surface Science, Vol. 603 (2009) 1841–1852.
- [6] T. Ramanathan, et al., *Functionalized graphene sheets for polymer nanocomposites*, Nature Nanotechnology, Vol. 3 (2008) 327–331.
- [7] P. J. Bryant, et al., *A study of mechanisms of graphite friction and wear*, Wear, Vol. 7 (1964) 118–126.
- [8] R. L. Fusaro, *A study of mechanisms of graphite friction and wear*, Wear, Vol. 53 (1979) 303–323.
- [9] J. Tian, et al., *The deintercalation effect of FeCl<sub>3</sub>-graphite intercalation compound in paraffin liquid lubrication*, Tribology International, Vol. 30 (1997) 571–574.
- [10] M. R. Hilton, et al., *Structural and tribological studies of MoS<sub>2</sub> solid lubricant films having tailored metal-multilayer nanostructures*, Surface Coating Technology, Vol. 53 (1992) 13–23.
- [11] J. Lin, et al., *Modification of graphene platelets and their tribological properties as a lubricant additive*, Tribology Letters, Vol. 41 (2011) 209–215.
- [12] B. Bhushan, et al., *Handbook of Tribology*, McGraw-Hill, New York, 1991.
- [13] W. Zhang, et al., *Tribological properties of oleic acid-modified graphene as lubricant oil additive*, Journal of Physics D: Applied Physics, Vol. 44 (2011) 205303.
- [14] H. D. Huang, et al., *An investigation on tribological properties of graphite nanosheets as oil additive*, Wear, Vol. 261 (2006) 140–144.
- [15] W. Hummers, et al., *Preparation of graphitic oxide*, Journal of the American Chemical Society, Vol. 80 (1958) 1339–1342.
- [16] *The history of Lonza's graphite powders*, Industrial Lubrication and Tribology, Vol. 27 (1975) 59–69.
- [17] C. Altavilla, P. Ciambelli, M. Sarno, M. R. Nobile, C. Gnerre, E. Somma, V. D'Agostino, A. Senatore, V. Petrone, *Tribological and rheological behaviour of lubricating greases with nanosized inorganic based additives*, Conference Proceedings of the 3rd European Conference on Tribology, Ecotrib 2011 and 4th Vienna International Conf. on Nanotechnology Viennano, Vienna 2011, 903–908.
- [18] M. Kalin, et al., *The Stribeck curve and lubrication design for non-fully wetted surfaces*, Wear, Vol. 267 (2009) 1232–1240.
- [19] M. H. Cho, et al. *Tribological properties of solid lubricants (graphite, Sb<sub>2</sub>S<sub>3</sub>, MoS<sub>2</sub>) for automotive brake friction materials*, Wear, Vol. 260 (2006) 855–860.
- [20] L. M. Malard, et al., *Raman spectroscopy in graphene*, Physic Reports, Vol. 473 (2009) 5–6.
- [21] A. C. Ferrari, et al., *Raman spectroscopy of graphene and graphite: Disorder, electron-phonon coupling, doping and nonadiabatic effects*, Solid State Communication, Vol. 143 (2007) 47–57.



- [22] M. A. Pimenta, et al., *Studying disorder in graphite-based systems by Raman spectroscopy*, Physical Chemistry Chemical Physics, Vol. 9 (2007) 1276–1291.
- [23] K. N. Kudin, et al., *Raman Spectra of Graphite Oxide and Functionalized Graphene Sheets*, Nano Letters, Vol. 8 (2008) 36–41.
- [24] L. Joly-Pottuz, et al., *Anti-wear and Friction Reducing Mechanisms of Carbon Nano-onions as Lubricant Additives*, Tribology Letters, Vol. 30 (2008) 69–80.
- [25] Y. Yao, et al., *Tribological property of onion-like fullerenes as lubricant additive*, Materials Letters, Vol. 62 (2008) 2524.
- [26] W. Zhao, et al., *Tribological properties of fullerenes C60 and C70 microparticles*, Materials Research, Vol. 11 (1996) 2749.
- [27] R. Rosentsveig, et al. *Fullerene-like MoS<sub>2</sub> Nanoparticles and Their Tribological Behavior*, Tribology Letters, Vol. 36 (2009) 175–182.
- [28] S. Brown, et al. *Bulk vs. Nanoscale WS<sub>2</sub>: Finite Size Effects and Solid-State Lubrication*, Nano Letters, Vol. 7 (2007) 2365.
- [29] V. Perfiliev, et al., *A new way to feed nanoparticles to friction interfaces*, Tribology Letters, Vol. 21 (2006) 89–93.
- [30] F. Abate, A. Senatore, V. D'Agostino, C. Leone, M. Sarno, P. Ciambelli, *Tribological properties of carbon nanotubes as lubricant additives*, Conference Proceedings of Nanotech Conference & Expo 2009, Houston, TX, United States, 2009, 3, 469.
- [31] X. C. Song, et al., *Hydrothermal synthesis and characterization of CNT@MoS<sub>2</sub> nanotubes*, Materials Letters, Vol. 60 (2006) 2346–2348.
- [32] M. Bar-Sadan, R. Tenne, *Inorganic Nanotubes and Fullerene-Like Structures – From Synthesis to Applications*, in: Inorganic Nanoparticles: Synthesis, Applications and Perspectives (Eds C. Altavilla, E. Ciliberto) CRC press, 2011, Chapter 16.
- [33] K. H. Hu, et al., *The effect of morphology on the tribological properties of MoS<sub>2</sub> in liquid paraffin*, Tribology Letters, Vol. 40 (2011) 155–165.
- [34] P. Ciambelli, C. Altavilla, M. Sarno, Y. Siraw, V. Petrone, A. Senatore, M. R. Nobile, E. Somma, C. Gnerre, *Tribological and rheological properties of tungsten disulphide nanosheets as additive in lubricant mineral oil*, Conference Proceedings of Int. Conference on Nanotechnology and Nanomaterials NanotechItaly 2010, Veneto Nanotech, Venezia, 2010, 177.
- [35] C. M. Praveen Kumar, et al., *Preparation and corrosion behavior of Ni and Ni-graphene composite coatings*, Materials Research Bulletin, Vol. 48 (2013) 1477–1483.
- [36] H. J. Song, et al., *Frictional behavior of oxide graphene nanosheets as water-base lubricant additive*, Applied Physics A: Materials Science & Processing, Vol. 105 (2011) 827.
- [37] V. Eswaraiyah, et al., *Graphene-based engine oil nanofluids for tribological applications*, ACS Applied Materials & Interfaces, Vol. 3 (2011) 4221.
- [38] L. Jinshan, et al., *Modification of graphene platelets and their tribological properties as a lubricant additive*, Tribology Letters, Vol. 41 (2011) 209.
- [39] T. Chen, et al., *Synthesis, characterization, and tribological behavior of oleic acid capped graphene oxide*, Journal of Nanomaterials, Vol. 2014 (2014) 654145.
- [40] A. H. Church, et al. *Carbon nanotube-based adaptive solid lubricant composites*, Advanced Science Letters, Vol. 5–1 (2012) 188–191.
- [41] L. Shu, et al., *Influence of adding carbon nanotubes and graphite to Ag-MoS<sub>2</sub> composites on the electrical sliding wear properties*, Acta Metallurgica Sinica, Vol. 23–1 (2010) 27–34.
- [42] X. Zhang, et al., *Carbon nanotube-MoS<sub>2</sub> composites as solid lubricants*. ACS Applied Materials & Interfaces, Vol. 1(3) (2009) 735–739.
- [43] K. Miura, *Encyclopedia of Nanoscience and Nanotechnology*, Vol. 9, American Scientific Publishers, Valencia, CA, 2004.
- [44] Q. Wang, et al., *Facilitated lithium storage in MoS<sub>2</sub> overlayers supported on coaxial carbon nanotubes*, The Journal of Physical Chemistry C, Vol. 111 (2007) 1675–1682.
- [45] S. J. Ding, et al., *Growth of MoS<sub>2</sub> nanosheets on CNTs for lithium storage*, Chemistry - A European Journal, Vol. 17 (2011) 13142–13145.
- [46] K. Jeong-Hui, et al., *The electrochemical properties of Li/TEGDME/MoS<sub>2</sub> cells using multi-wall carbon nanotubes as a conducting agent*, Research on Chemical Intermediates, Vol. 36 (2010) 749.
- [47] A. B. Laursen, et al., *Molybdenum sulfides-efficient and viable materials for electro- and photoelectrocatalytic hydrogen evolution*, Energy & Environmental Science, Vol. 5 (2012) 5577.
- [48] J. Li, et al., *The effect of CNT modification on the mechanical properties of polyimide composites with and without MoS<sub>2</sub>*, Mechanics of Composite Materials, Vol. 47 (2011) 597.
- [49] M. Levy, et al., *Synthesis of inorganic fullerene-like nanostructures by concentrated solar and artificial light*, Israel Journal of Chemistry, Vol. 50 (2010) 417.

- [50] X. C. Song, et al., *Hydrothermal synthesis and characterization of CNT@MoS<sub>2</sub> nanotubes*, Materials Letters, Vol. 60 (2006) 2346–2348.
- [51] L. Ma, et al., *Carbon nanotubes coated with tubular MoS<sub>2</sub> layers prepared by hydrothermal reaction*, Nanotechnology, Vol. 17 (2006) 571.
- [52] V. O. Koroteev, *Growth of MoS<sub>2</sub> layers on the surface of multiwalled carbon nanotubes*, Inorganic Materials, Vol. 43 (2007) 236.
- [53] H. Shang, et al., *States of carbon nanotube supported Mo-based HDS catalysts*, Fuel Processing Technology, Vol. 88 (2007) 117.
- [54] C. Altavilla, et al., *New “chimie douce” approach to the synthesis of hybrid nanosheets of MoS<sub>2</sub> on CNT and their anti-friction and anti-wear properties*, Nanotechnology, Vol. 24 (2013) 125601.
- [55] C. Altavilla, M. Sarno, P. Ciambelli, Pat. No. WO 2012042511A1 20120405.
- [56] V. D'Agostino, et al., *Effects of the piezoviscous lubricant properties on EHL line and point contact problems*, Tribology Letters, Vol. 49–2 (2013) 385–396.
- [57] A. Senatore, et al., *Advances in piston rings modelling and design*, Recent Patents on Engineering, Vol. 7–1 (2013) 51–67.
- [58] L. Joly-Pottuz, et al., *Friction properties of carbon nano-onions from experiment and computer simulations*, Tribology Letters, Vol. 37–1 (2010) 75–81.
- [59] O. Tevet, et al., *Nanocompression of individual multilayered polyhedral nanoparticles*, Nanotechnology, Vol. 21 (2010) 365705.
- [60] O. Tevet, et al., *Friction mechanism of individual multilayered nanoparticles*, Proceedings of the National Academy of Sciences, Vol. 108–50 (2010) 19901.
- [61] G. Seifert, et al., *Structure and electronic properties of MoS<sub>2</sub> nanotubes*, Physical Review Letters, Vol. 85 (2000) 146–149.
- [62] B. Derjaguin, et al., *Electrostatic component of the rolling friction force moment*, Wear, Vol. 7 (1964) 270–281.
- [63] G. Liu, et al., *Investigation of the Mending Effect and Mechanism of Copper Nanoparticles on a Tribologically Stressed Surface*, Tribology Letters, Vol. 17–4 (2004) 961–966.
- [64] F. Dassenoy, et al., *Carbon nanotubes as advanced lubricant additives*, in: Carbon Nanotubes, V. N. Popov and P. Lambin, Eds., vol. 222 of NATO Science Series II: Mathematics, Physics and Chemistry, pp. 237–238, 2006.



#### НОВИ МОДИФИКАТОРИ ТРЕЊА НАНО-ВЕЛИЧИНЕ ЗА МАЗИВА ЗА МОТОРЕ, РЕДУКТОРЕ И ВАЉКАСТЕ ЛЕЖАЈЕВЕ

**Сажетак:** У овом раду приказане су триболошке карактеристике нанослојева графеновог оксида у минералним уљима у широком спектру услова, од граничне и мјешовите лубриације до еластохидронамичких окружења. У групу I минералних уља распршени су нанослојеви графеновог оксида припремљени модификованом Hummer-овом методом. Формулисани лубрикант тестиран је путем кугле на трибометру с диском како би се измјерило смањење трења у односу на основно минерално уље. Добре особине које мјешавина графена и уља има у смислу трења и хабања могу се евентуално приписати ситној структури нанослојева и њиховој екстремно ламинираној структури, који смањују посимично напрезање и спречавају међудејство неравнина метала у примјени мотора као и окружењу редуктора. Резултати недвосмислено показују да графенске тракице у уљу лако формирају заштитни слој и тако спречавају директан контакт између површина челика, побољшавајући карактеристике основног уља у погледу трења. Овај доказ је такође повезан са тенденцијом коефицијента трења у граничном режиму. Такође, хибридни органски и-неоргански нанокомпозици су успјешно тестирани као адитиви којим се смањује трење и хабање код мазива као потенцијалне средине пробоја у примјени ваљкастих лежајева.

**Кључне ријечи:** графенов оксид, нанослојеви, модификатор трења нано-величине, смањење хабања, мазиво (лубрикант), хибридни наноадитиви.

